

OPEN

MicroRNA-205-5p inhibits skin cancer cell proliferation and increase drug sensitivity by targeting TNFAIP8

Xinhong Ge^{1,2,5}, Suryakant Niture^{2,5}✉, Minghui Lin³, Patrice Cagle², P. Andy Li⁴ & Deepak Kumar²✉

Tumor necrosis factor- α -induced protein 8 (TNFAIP8) is a member of the TIPE/TNFAIP8 family which regulates tumor growth and survival. Our goal is to delineate the detailed oncogenic role of TNFAIP8 in skin cancer development and progression. Here we demonstrated that higher expression of TNFAIP8 is associated with basal cell carcinoma (BCC), squamous cell carcinoma (SCC), and melanoma development in patient tissues. Induction of TNFAIP8 expression by TNF α or by ectopic expression of TNFAIP8 in SCC or melanoma cell lines resulted in increased cell growth/proliferation. Conversely, silencing of TNFAIP8 decreased cell survival/cell migration in skin cancer cells. We also showed that miR-205-5p targets the 3'UTR of TNFAIP8 and inhibits TNFAIP8 expression. Moreover, miR-205-5p downregulates TNFAIP8 mediated cellular autophagy, increased sensitivity towards the B-RAF^{V600E} mutant kinase inhibitor vemurafenib, and induced cell apoptosis in melanoma cells. Collectively our data indicate that miR-205-5p acts as a tumor suppressor in skin cancer by targeting TNFAIP8.

Skin cancer is currently one of the most common types of malignancy^{1,2}. In the United States alone, more than 9500 people are diagnosed with skin cancer every day and more than two people die of the disease every hour (Skin cancer facts and statistics: 2019, <https://skincancer.org/skin-cancer-information/skin-cancer-facts/>: Accessed November 14, 2019)^{3,4}. Caucasians are 20 times more likely to be diagnosed with skin cancer than African Americans. Skin cancers exist in several forms and therefore early diagnosis and treatment is a significant challenge⁵. Skin cancers include malignant melanoma (MM) and non-melanoma skin cancers (NMSC)⁶, and the most common non-melanoma skin cancers are squamous cell carcinoma (SCC) and basal cell carcinoma (BCC)⁶.

Ultraviolet radiation (UV), environmental pollutants, chemical carcinogens, and work-related exposures are known to increase the risk of skin cancer⁷⁻⁹. A variety of molecular mechanisms associated with the development of skin cancer also have been described^{10,11}. Exposure of UVA induces the expression of Autophagy Receptor Adaptor p62 protein in melanocytes and p62 acts as an oncogene in UVA-associated melanoma development and progression¹². Analysis of whole-genome landscapes of major melanoma subtypes has identified several key gene mutations in cutaneous melanoma, including *B-RAF*, *CDKN2A*, *NRAS*, in acral melanoma *TP53*, *B-RAF*, *NRAS* and *NFL* and *SF3B1* in mucosal melanoma¹³. The study further revealed that these mutations are not correlated with alternative telomere lengthening but associated with greater telomere length and also modulates the MAPK and PI3K pathway in melanomas¹³. Moreover, during melanoma development, several somatic alterations activate the MAPK and PI3K pathway, upregulate telomerase activity, modulate chromatin landscape, override the G1/S checkpoint, the ramp-up of MAPK signaling, and disrupt the p53 pathway¹⁴. In melanoma, activation of several oncogenes including *RAS*, *B-RAF*, *Cyclin D1*, *CDK2*, *c-MYC*, *HDM2*, *MAPK1/2*, *ERBB4*, *GRIN2A*, *GRM3*, *RAC1*, and *PREX2* were reported previously^{15,16}.

¹Department of Dermatology, General Hospital of Ningxia Medical University, Yinchuan 750004, Ningxia Hui Autonomous Region, China. ²Julius L. Chambers Biomedical Biotechnology Research Institute (BBRI), North Carolina Central University, 1801 Fayetteville St., Durham, NC 27707, USA. ³Department of Respiratory Diseases, The Fourth People's Hospital of Ningxia Hui Autonomous Region, Yinchuan 750021, Ningxia Hui Autonomous Region, China. ⁴Department of Pharmaceutical Sciences, Bio-Manufacturing Research Institute and Technology Enterprise (BRITE), College of Health and Sciences, North Carolina Central University, Durham, NC 27707, USA. ⁵These authors contributed equally: Xinhong Ge and Suryakant Niture. ✉email: sniture@nccu.edu; dkumar@nccu.edu

microRNAs (miRNAs) have been shown to regulate key pathways in skin cancer. miRNAs are small single-stranded non-coding RNAs that modulate post-transcriptional gene expression by binding to the 3' untranslated regions (3'UTRs) of target mRNAs. The binding of miRNAs to 3'UTRs of target mRNA regulates both the stability and translation of mRNA transcripts and thus affects gene expression¹⁷. Reports suggest that by directly targeting key gene expression, miRNAs modulate various cellular processes such as cell proliferation/survival, cell-cycle control, cell apoptosis, the stress response, cell metabolism, development, and differentiation^{18,19}. In melanoma, the expression of several miRNAs are upregulated, for example, miR-214, miR-30b, miR-30d, miR-506, miR-514, miR-21, miR-155, and miR-221. These microRNAs promote melanoma cell growth and proliferation by acting as oncogenes^{20–24}. On the other hand, studies also demonstrate that miR-29c, miR-34b, miR-375, and miR-205, are downregulated in melanoma and behave as tumor suppressors^{19,25–28}.

Tumor necrosis factor- α -induced protein 8 (TNFAIP8) is also known as SCC-S2, GG2-1, and NDED. TNFAIP8 is a member of the TNFAIP8/TIPE family which has three other members designated as TNFAIP8-like protein 1 (TIPE1), TNFAIP8-like protein 2 (TIPE2), and TNFAIP8-like protein 3 (TIPE3)^{29–32}. TNFAIP8 is a tumor necrosis factor-alpha (TNF α) inducible protein^{33–35}. Moreover, the expression of TNFAIP8 is also controlled by several transcriptional factors including nuclear factor- κ B (NF- κ B), androgen receptor (AR), p53, and orphan nuclear receptor chicken ovalbumin upstream promoter transcription factor I (COUP-TFI)^{32,35–37}. TNFAIP8 also regulates inflammation, immunity, and involved in several human diseases³⁶. TNFAIP8 is known to regulate several genes associated with cell proliferation (*IL-24*, *FAT3*, *LPHN2*, *EPHA3*), fatty-acid oxidation (*ACADL*), and several oncogenes, for example, *NFAT5*, *MALAT1*, *MET*, *FOXA1*, *KRAS*, *S100P*, *OSTF1*³⁵. TNFAIP8 has been shown to inhibit cell apoptosis and increase cell proliferation in numerous cancers including lung cancer^{38–41}, liver cancer^{42,43}, gastric cancer⁴⁴, esophageal cancer (ESCC)^{45,46}, pancreatic cancer⁴⁷, and prostate cancer^{32,34,35}. Here we extend the analysis of the oncogenic role of TNFAIP8 and investigate the role TNFAIP8 in skin cancer cell proliferation/survival and progression. Our data suggest that overexpression of TNFAIP8 promotes cell survival and cell colony formation/cell growth in skin cancer cells. Further, we demonstrated that miR-205-5p controls TNFAIP8 expression and reduces skin cancer cell survival, and increases sensitivity to the B-RAF $V600E$ mutant kinase inhibitor vemurafenib in melanoma cells.

Results

Expression of TNFAIP8 is higher in skin cancer tissues. To investigate the pathological role of TNFAIP8 in skin cancer progression, we first analyzed the expression of TNFAIP8 in BCC, SCC, and melanoma by immunohistochemistry in human skin cancer patient tissue samples. The expression of TNFAIP8 was found to be significantly increased in BCC (n=6) and low/medium differentiated SCC tissue (n=4) compared with normal skin tissues (n=6) (Fig. 1A,B). The expression of TNFAIP8 was not significantly altered in highly differentiated SCC compared with normal skin tissue. Interestingly, the expression of TNFAIP8 was significantly increased (~ two fold) in melanoma tissues compared with normal skin tissues (Fig. 1A,B). Also, we analyzed the TNFAIP8 mRNA expression between cutaneous melanoma (n=45) and melanoma precursor (n=18) samples as reported in the Oncomine dataset (<https://www.oncomine.org/resource/login.html> accessed October 17, 2020)⁴⁸ (Fig. 1C). The data suggest that the expression of TNFAIP8 transcripts is 2.55-fold higher in melanoma precursor tissues compared with cutaneous melanoma (Fig. 1C). Collectively, our data suggest that TNFAIP8 expression is higher in skin cancer and melanoma tissues.

To establish the role of TNFAIP8 in skin cancer, we compared the expression of TNFAIP8 in normal human skin cell line HaCaT (B-RAF wild) to human skin cancer cell lines, including the epidermoid squamous cell carcinoma A431 (B-RAF wild) and melanoma cell lines A375, A2058 (B-RAF $V600E$ mutant) and SK-MEL-2 (B-RAF wild) cells. First, we analyzed the expression of B-RAF wild and B-RAF $V600E$ mutant proteins in these cell lines (Fig. 1D). Consistent with earlier reports, immunoblotting data from our laboratory indicate that all the skin cancer cell lines and normal skin cells used in this study expressed moderate levels of either B-RAF wild-type protein in HaCaT, A431, SK-MEL-2 cells, or B-RAF $V600E$ mutant protein in A375 and A2058 cells (Fig. 1D)^{49,50}. Further, we analyzed the expression of TNFAIP8 protein and transcripts in normal skin cells and B-RAF wild type or B-RAF $V600E$ mutant skin cancer cells (Fig. 1E,F). Immunoblotting and RT/qPCR data demonstrated that TNFAIP8 expression was higher in SK-MEL-2 (melanoma cells), A431 (SCC cells), and HaCaT (normal skin cells) which express B-RAF wild type protein, and lower expression of TNFAIP8 was observed in A375 and A2058 melanoma cells that expressed B-RAF $V600E$ mutant protein (Fig. 1E,F).

B-RAF protein is a serine-threonine kinase and mutation of B-RAF $V600E$ increases approximately 500-fold kinase activity compared with wild-type B-RAF in 27–70% of melanoma cancer. B-RAF $V600E$ mutant protein is constitutively active⁵¹ and earlier studies demonstrated that B-RAF $V600E$ mutant dysregulates NF- κ B/Snail/RKIP/PTEN circuit as well as activates MEK/ERK kinases that promote the epithelial to mesenchymal transition (EMT) and melanoma cell growth^{51,52}. Since NF- κ B regulates the expression of TNFAIP8, the exact role of B-RAF $V600E$ mutant in the regulation of TNFAIP8 expression transcriptionally or post-transcriptionally through NF- κ B is not clear, however, our data suggest that mutant B-RAF $V600E$ downregulates the expression of TNFAIP8 (mRNA) as well as decreases the level/stability of TNFAIP8 protein in A375 and A2058 melanoma cells. This needs to be further investigated.

TNF α regulates the expression of TNFAIP8 and skin cancer cell survival. The classical model of TNFAIP8 regulation suggests that cytokine TNF α binds with TNF α 1/2 receptors and induced cellular inflammation. This leads to dissociations of transcription factor NF- κ B from its inhibitor IKK β , NF- κ B translocates into the nucleus, binds with TNFAIP8 promoter, and induced TNFAIP8 expression³². Reports also suggest that TNFAIP8 gene expressed several protein variants/isoforms in cancer cell lines^{34,35}, and therefore first we analyzed the expression TNFAIP8 isoforms in normal and skin cancer cells by RT/PCR (Fig. 2A,B). SCC-A431 and

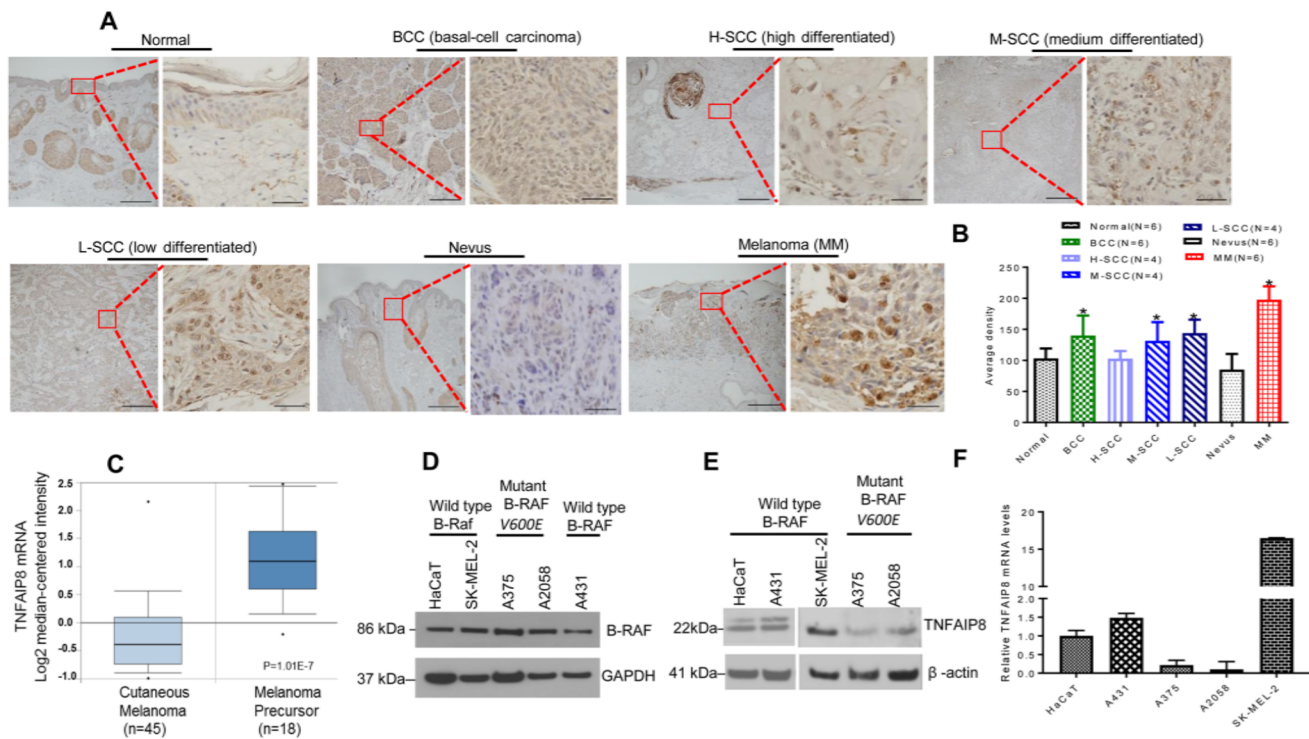


Figure 1. TNFAIP8 expression is upregulated in BCC, SCC, and melanoma patient skin tissues. **(A)** Relative immunohistochemical TNFAIP8 expression in indicated skin cancer tissues is presented. **(B)** Immunohistochemical expression levels of TNFAIP8 protein from normal skin (n = 6), BCC (n = 6), H-SCC (n = 4), M-SCC (n = 4), L-SCC (n = 4), nevus (n = 6), and melanoma (n = 6) tissues were quantified using ImageJ software (<https://imagej.nih.gov/ij/>) and plotted. The data represent mean \pm SEM from 4 to 6 skin cancer tissues. *P < 0.05 relative to normal skin tissues. **(C)** Expression of TNFAIP8 transcripts between cutaneous melanoma (n = 45) and melanoma precursor (n = 18) samples were analyzed and presented from the Oncomine dataset (<https://www.oncomine.org/resource/login.html> accessed October 17, 2020). ***P < 0.001 relatives to cutaneous melanoma tissues. **(D, E)** Expression of wild-type B-RAF, mutant B-RAF^{V600E}, and TNFAIP8 in HaCaT, SK-MEL-2, A431, A375, and A2058 cells were analyzed by western blotting. Fifty micrograms of lysates from normal and skin cancer cells were immunoblotted with B-RAF, TNFAIP8, GAPDH, and β-actin antibodies. Immunoreactive bands were visualized using ECL chemiluminescence detection reagents after exposing the blots on X-ray films (**D**) or by scanning the blots with an Odyssey CLX Imager (**E**). The immunoblot scans were converted into grayscale and presented. **(F)** Expression of TNFAIP8 mRNA from indicated normal skin cells and skin cancer cells were analyzed by RT/qPCR as described in the “Materials and methods” section.

melanoma cells expressed isoform two predominantly but not in normal HaCaT cells. Normal HaCaT cells, A431, A375, A2058 cells expressed isoform one, whereas expression of isoform one is not observed in SK-MEL-2 cells suggesting that, skin cancer cells expressed isoform two predominantly (Fig. 2B) and the involvement of TNFAIP8 variant/isoform 2 in lung cancer and liver cancer development and progression has been reported earlier^{37,43}.

Further, to test whether TNFα induced expression of TNFAIP8 in skin cancer cells, we treated normal and skin cancer cells with TNFα (10–50 ng/ml), and the induction of TNFAIP8 protein and mRNA were analyzed (Fig. 2C,D). Treatment of TNFα (10–20 ng/ml) induced the expression of TNFAIP8 protein in normal HACaT skin cells as well as in skin cancer cell lines (Fig. 2C). Consistent with immunoblotting data, the relative mRNA expression of TNFAIP8 was also increased by 1–2.7 fold in HaCaT, A431, A375, and A2058 cell lines when cells treated with TNFα (10–20 ng/ml), whereas, the expression of TNFAIP8 was decreased at higher concentration of TNFα (50 ng/ml) (Fig. 2D). Interestingly, B-RAF mutant A375 and A2058 melanoma cell lines which expressed lower levels of TNFAIP8, upon a dose-dependent treatment with TNFα (10–50 ng/ml) induced TNFAIP8 protein expression (Fig. 2C) suggesting that TNFα induced TNFAIP8 expression in normal and skin cancer cell lines irrespective B-RAF background. Since TNFAIP8 modulates cell survival/proliferation in several cancer cell lines, the role of TNFα mediated induction of TNFAIP8 in skin cancer cell survival was analyzed by MTT assay (Fig. 2E). The data suggest that induction of TNFAIP8 by TNFα (10–20 ng/ml) increased cell survival in normal HaCaT cells as well as in A431 cells and A375, A2058 melanoma cell lines significantly, whereas, a higher concentration of TNFα (50 ng/ml) treatment decreased cell survival in A431, A375 and A2058 skin cancer cell lines (Fig. 2E). We also analyzed the time-dependent effect of TNFα (20 ng/ml) on the expression of TNFAIP8 and cell survival (Supplementary Fig. S1A,B). Our data suggest that treatment of TNFα (20 ng/ml) increased TNFAIP8 expression and cell survival after 12–24 h and significantly decreased the TNFAIP8 expression and cell survival after 48 h treatment (Supplementary Fig. S1A,B) suggesting that, TNFα regulates the expression of TNFAIP8 and cell survival in skin cancer cells with a time-dependent manner.

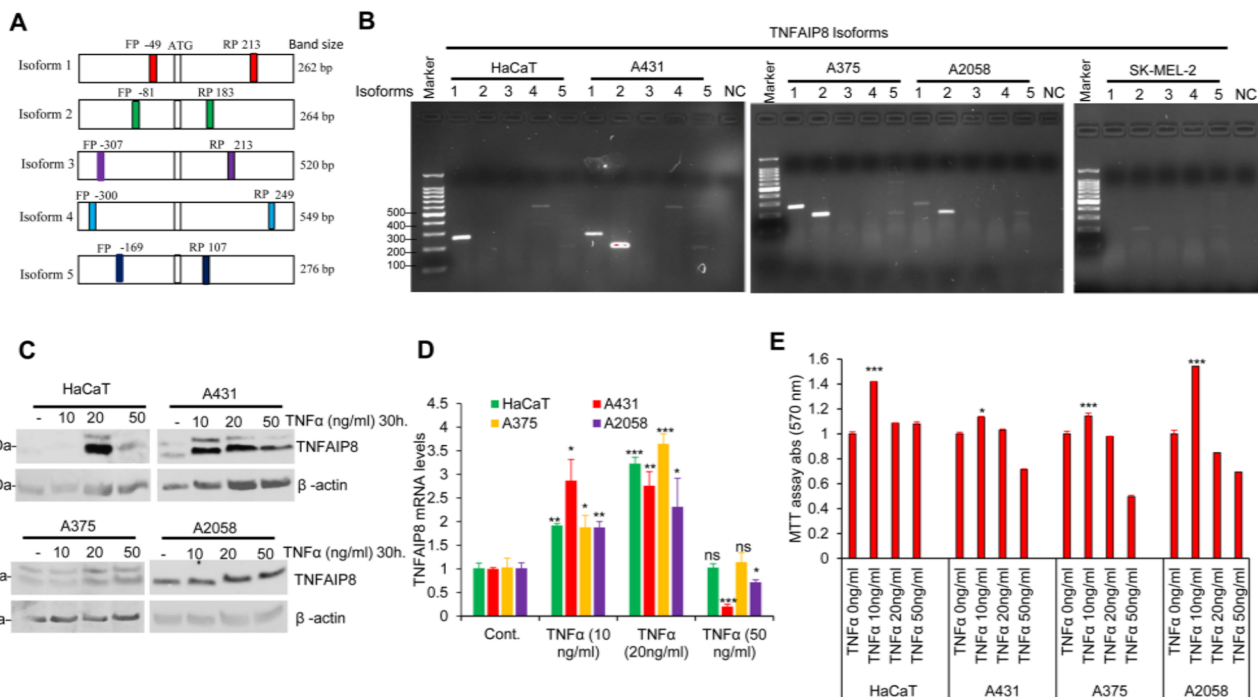


Figure 2. TNF α -induced TNFAIP8 expression in skin cancer cells **(A)** Schematic represents TNFAIP8 isoform-specific forward and reverse primer design. **(B)** The expression of different variants/isoforms of TNFAIP8 in normal HaCaT and skin cancer cells was analyzed by RT-PCR. NC—negative control (no cDNA). **(C)** HaCaT, A431, A375, and A2058 cells were treated with vehicle or TNF α (10–50 ng/ml) for 30 h, and cell lysates were immunoblotted with TNFAIP8 or β -actin antibodies. Immunoreactive bands were visualized using ECL chemiluminescence detection reagents and the blots were scanned using an Odyssey CLx imager. The immunoblot scans were converted into grayscale and presented. **(D)** Similarly, normal and skin cancer cells were treated with vehicle or TNF α (10–50 ng/ml) for 30 h, and TNFAIP8 mRNA expression was analyzed by RT/qPCR as described in the “Materials and methods” section. * P <0.05, ** P <0.01, *** P <0.001 relative to control/vehicle-treated cells. **(E)** HaCaT, A431, A375 and, A2058 cells were treated with vehicle or TNF α (10–50 ng/ml) for 48 h and, relative cell survival was analyzed by MTT assay as described in the “Materials and methods” section. Results are representative of three independent experiments. * P <0.05, *** P <0.001 relative to control/vehicle-treated cells.

Overexpression of TNFAIP8 increases skin cancer cell survival, colony formation and migration. To clarify the exact role of TNFAIP8 in skin cancer cell proliferation, we transiently transfected normal HaCaT skin cells and A431, A375, and A2058 skin cancer cells with empty vector (EV) or TNFAIP8-Myc plasmid (Fig. 3A). Immunoblotting data demonstrated the overexpression of TNFAIP8-Myc tagged protein in cells transfected with TNFAIP8-Myc tagged plasmid but not in an empty vector (EV) transfected cells (Fig. 3A). The MTT assay demonstrated that overexpression of TNFAIP8 increased cell survival significantly; by ~55%, 82%, 68% in A431, A375, and A2058 skin cancer cells, respectively (Fig. 3B). However, no significant effect on cell survival/proliferation was observed in HaCaT normal skin cells transfected with TNFAIP8 (Fig. 3B). We also examined the effect of TNFAIP8 overexpression on skin cancer cell colony formation ability. TNFAIP8 expression promoted cell colony formation in A431 cells by 3.1-fold, A375 cells by 4.2-fold, and A2058 cells by 5.1-fold compared with empty vector-transfected cells (Fig. 3C, upper and lower panels). Similarly, no significant effect of TNFAIP8 overexpression on cell colony formation was observed in normal skin HaCaT cells (Fig. 3C, upper and lower panels). These results suggest that TNFAIP8 overexpression promotes cell growth in skin cancer cells but not in normal skin cells.

In parallel, we used siRNA to knockdown endogenous TNFAIP8 protein in normal and skin cancer cells (Fig. 3D). Transfection of TNFAIP8 siRNA significantly reduced endogenous TNFAIP8 levels in all cell lines compared with the control siRNA transfected cells (Fig. 3D). The effect of TNFAIP8 knockdown on cell survival was then analyzed by MTT assay. MTT assay demonstrated that TNFAIP8 knockdown reduced cell survival in A431 cells by 22%, in A375 cells by 55.2%, and in A2058 cells by 45.3% compared with control siRNA transfected cells (Fig. 3E). Similarly, TNFAIP8 knockdown also significantly decreased cell colony formation ability in A431 cells by 18.4%, in A375 cells by 53.2%, and in A2058 cells by 40.3% compared with control siRNA transfected cells (Fig. 3F, upper and lower panels). Also, we evaluated the effect of TNFAIP8 knockdown on skin cancer cell migration using wound healing migration assay. The wound healing migration assay revealed that TNFAIP8 knockdown significantly inhibited cell migration and wound closure in A431 (15.1%), A375 (52.5%), and A2058 (70.4%) compared with control siRNA transfected cells (Fig. 3G, upper and lower panels). In contrast, no significant effects on cell survival, cell colony formation, and migration were observed in HaCaT cells transfected

with TNFAIP8 siRNA compared with control siRNA transfected cells (Fig. 3E–G). Indeed, the data presented in Fig. 3 suggests that TNFAIP8 promotes cell proliferation and cell migration in skin cancer cells.

miR-205-5p targets the TNFAIP8-3'UTR and inhibits TNFAIP8 expression. In a previous study, it was reported that miR-205-5p targets the 3'-UTR of either transcription factor E2F1 or transcription factor E2F5 and suppresses the cell proliferation in melanoma cells²⁸. Since our data show that TNFAIP8 promotes skin cancer cell survival and migration, we searched for miRNAs that possibly target TNFAIP8 gene expression. TargetScan, an online software tool (http://www.targetscan.org/vert_72/; accessed June 10, 2019), was used to predict and identify possible 3' TNFAIP8-UTR binding miRNAs. TargetScan analysis revealed that miR-205-5p is predicted to bind with the 3' UTR of *TNFAIP8* gene (61–68) (Fig. 4A). To analyze the effect of miR-205-5p on TNFAIP8 expression, first, we determined the endogenous expression levels of miR-205-5p in HaCaT cells and skin cancer cells. RT/qPCR data showed that miR-205-5p expression was higher in HaCaT cells and SCC-A431 cells, whereas, the expression of miR-205-5p was not detected in melanoma A375, A2058, and SK-MEL-2 (Fig. 4B). To determine whether miR-205-5p binds directly with the TNFAIP8-3'UTR, we performed a TNFAIP8-3'UTR luciferase assay. A431 and A2058 cells were co-transfected with TNFAIP8-3'UTR-Luc plasmid for 18 h and then cells were transfected miR-205-5p mimic or mutant miR-205-5p mimic for 30 h and luciferase activity was determined. The data showed that the miR-205-5p mimic significantly inhibited luciferase activity compared with negative control (NC) or mutant miR-205-5p mimic transfected both cell lines (Fig. 4C). These results support the model where the miR-205-5p mimic binds with the TNFAIP8-3'UTR.

To determine whether the miR-205-5p mimic represses the endogenous expression of TNFAIP8 mRNA and protein, we transfected normal HaCaT cells, A431 (SCC) and A2058 melanoma cells with miR-205-5p mimic or negative control (NC). Overexpression of miR-205 mimic in HaCaT, A431, and A2058 cell lines was analyzed by RT/qPCR (Fig. 4D). Overexpression of miR-205-5p mimic significantly decreased both TNFAIP8 mRNA and protein expression in HaCaT, A431 and A2058 cell lines (Fig. 4E,F). We also performed immunocytochemistry and analyzed endogenous TNFAIP8 protein expression by immunofluorescence after delivery of Cy3 labeled miR-205-5p or Cy3 labeled NC mimic into HaCaT, A431 and A2058 cells (Fig. 4G). TNFAIP8 immunofluorescence data suggest that transfection of Cy3-miR-205-5p in all three cell lines decreased cytosolic TNFAIP8-associated fluorescence (merge panel) compared with Cy3-labeled-NC mimic transfected cells (Fig. 4G) suggesting that miR-205-5p targets the TNFAIP8-3'UTR and inhibits TNFAIP8 protein expression.

miR-205-5p inhibits cell survival and TNFAIP8-mediated autophagy induction. Since miR-205-5p inhibits TNFAIP8 expression and TNFAIP8 promotes cell proliferation in skin cancer cells, we further examined the role of miR-205-5p mimic in the regulation of skin cancer cell survival/cell colony formation. No significant effect on cell proliferation/survival was observed in HaCaT cells transfected of miR-205-5p or the NC mimic control, however, a significant decrease in cell proliferation was observed in A431 and A2058 cell lines (Fig. 5A). Also, we analyzed the effect of miR-205-5p on cell colony formation in normal skin cell line HaCaT, and A431 and A2058 cell lines (Fig. 5B). Similar to the effects were seen in the cell survival assay, transfection with miR-205-5p mimic or the NC mimic control did not affect cell colony formation in HaCaT cells (Fig. 5B, left panel). Interestingly, cell colony formation was decreased by 32.5% in A431 cells and 38.5% in A2058 cells when cells were transfected with miR-205-5p compared with NC transfected cells (Fig. 5B, middle and right panels).

In a previous study, we showed that TNFAIP8 induced autophagy in prostate, breast, and liver cancer cells and increased resistance to specific anti-cancer drugs^{34,43}. Consistent with these findings, we demonstrate here that overexpression of TNFAIP8 also induced autophagy in HaCaT, A431, and A2058 cell lines based on induction of autophagy bio-marker LC3 β II (Fig. 5C). Conversely, inhibition of TNFAIP8 expression by miR-205-5p mimic decreased autophagy biomarkers LC3 β II and p62 expression in A431 and A2058 cells compared with NC mimic control transfected cells (Fig. 5D). To support this, we also performed immunocytochemistry and analyzed the effect of miR-205-5p mimic on LC3 β -related puncta formation in skin cancer cells. Immunocytochemistry data showed that miR-205-5p mimic transfection significantly decreased LC3 β related puncta formation in A431 and A2058 cells as well as in HaCaT cells (Fig. 5E, upper and lower panels) suggesting that miR-205-5p inhibits cell proliferation and TNFAIP8-mediated autophagy induction in skin cancer cells.

miR-205-5p increases the sensitivity of skin cancer cells to vemurafenib. Currently, vemurafenib and paclitaxel drugs are used as combine chemotherapy for the treatment of skin cancer patients affected by advanced melanoma which express B-RAF^{V600E} mutant protein⁵³. We treated HaCaT and SK-MEL-2 cells which possess wild type B-RAF protein, and A375 and A2058 cells which express mutant B-RAF^{V600E} with vemurafenib and relative drug sensitivity were analyzed by cell survival MTT assay (Fig. 6A). Consistent with the clinical data, a dose-dependent treatment of vemurafenib (0.1–25 μ M) decreased cell survival in A375 and A2058 which possesses B-RAF^{V600E} mutant, whereas, SK-MEL-2 cells and HaCAT cell lines which express wild type B-RAF protein showed significant resistance to vemurafenib (Fig. 6A).

Since the expression miR-205-5p was not detected in melanoma A375 and A2058 cell lines (Fig. 4B), and miR-205-5p targets TNFAIP8, we further examined the potential role of miR-205-5p in vemurafenib sensitivity. We transfected normal and skin cancer cells with miR-205-5p and treated with vemurafenib as indicated and relative drug sensitivity was analyzed (Fig. 6B). Compared with control NC mimic transfected cells, miR-205-5p transfection alone decreased cell survival in A375, and A2058 cells but not in HaCaT or SK-MEL-2 cells significantly (Fig. 6B). Transfection with miR-205-5p and treatment with vemurafenib further decreased cell survival compared with vemurafenib alone in skin cancer lines SK-MEL-2, A375, and A2058 cells (Fig. 6B, left and right panels). Interestingly, the data also indicated that B-RAF^{V600E} mutant cell lines A375 and A2058 showed

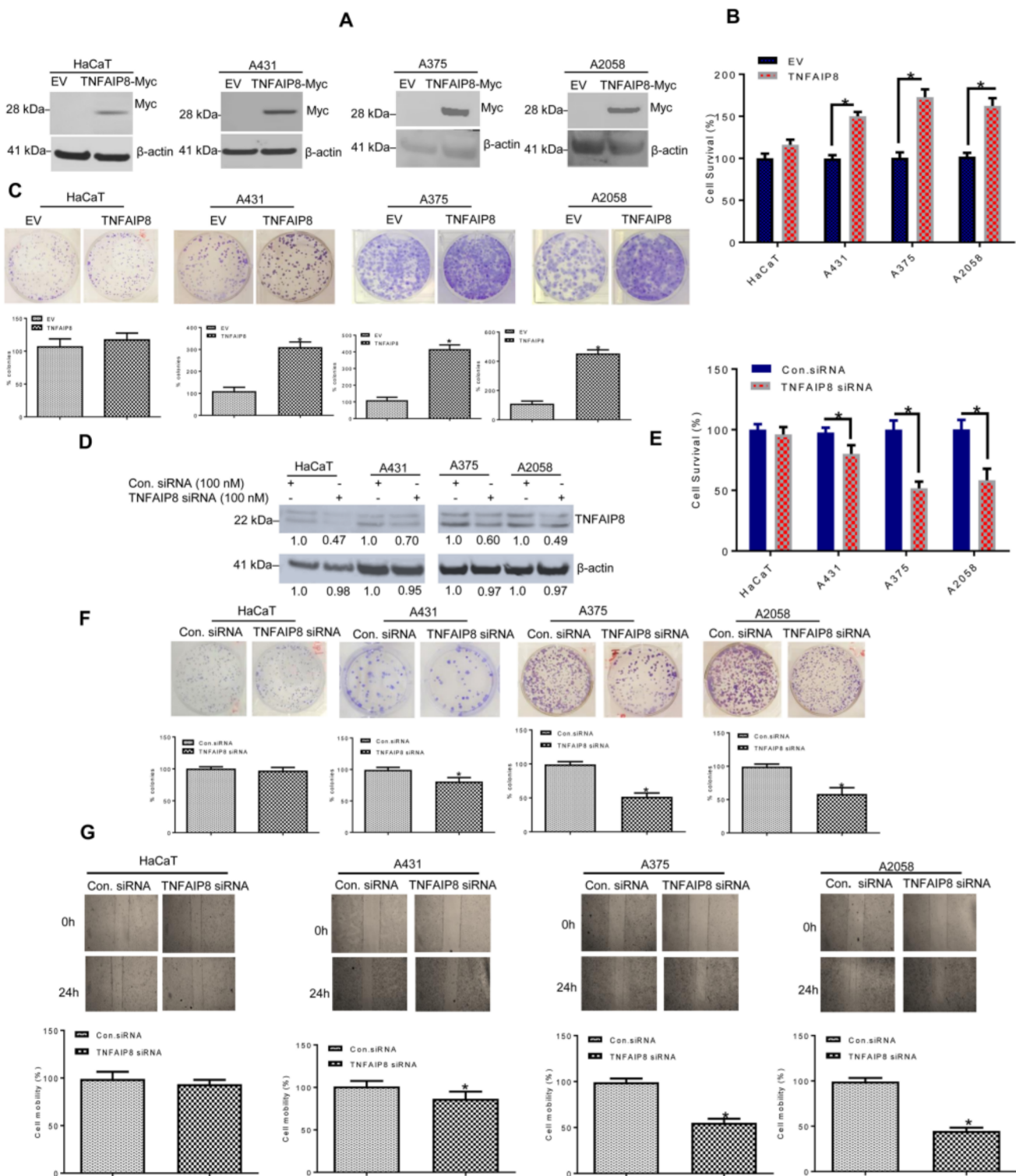


Figure 3. TNFAIP8 regulates cell proliferation and migration in skin cancer cells. (A) Western blotting analysis of TNFAIP8-Myc tagged protein expression in HaCaT and skin cancer cells. Immunoreactive bands were developed using ECL chemiluminescence detection reagents and the blots were scanned using an Odyssey CLx imager. The immunoblot scans were converted into grayscale and presented. (B) Effect of TNFAIP8-Myc protein overexpression on HaCaT, A431, A375 and, A2058 on cell survival was measured by MTT assay. Results are representative of three independent experiments. * $P < 0.05$ relative to EV transfected cells. (C) The effect of overexpression of TNFAIP8-Myc on cell colony formation was analyzed and plotted (upper and lower panels) as described in the “Materials and methods” section. * $P < 0.05$ relative to EV transfected cells. (D) HaCaT, A431, A375 and, A2058 cells were transfected with control siRNA or TNFAIP8 siRNA (100 nM) for 30 h, and cell lysates were western blotted with anti-TNFAIP8 and β -actin antibodies. Western blots were developed using ECL chemiluminescence detection reagents and the blots were scanned using an Odyssey CLx imager. The immunoblot scans were converted into grayscale and presented. TNFAIP8 and β -actin protein levels were quantified using ImageJ software (<https://imagej.nih.gov/ij/>) and presented below. (E) The effect of TNFAIP8 knockdown by siRNA on cell survival was analyzed by MTT assay. The experiments were independently performed three times. * $P < 0.05$ relative to control siRNA transfected cells. (F) Control siRNA and TNFAIP8 siRNA-transfected HaCaT, A431, A375 and A2058 cells (3000 cells/well) were re-plated in 6-well plates in triplicate for 7–10 days and skin cancer cell colony formation was analyzed and plotted (upper and lower panels) as described in the “Materials and methods” section. * $P < 0.05$ relative to control siRNA transfected cells. (G) Wound healing assay: HaCaT, A431, A375 and A2058 cells were transfected with control siRNA or TNFAIP8 siRNA for 48 h. The effect of the TNFAIP8 knockdown on cell migration was analyzed using the wound healing assay. Representative images of the wound healing assay (top) and the calculated scratch area (bottom) are shown. * $P < 0.05$ relative to control siRNA transfected cells.

increased sensitivity to vemurafenib treatment after transfection with miR-205-5p compared with B-RAF wild protein-expressing cell lines. Thus, by targeting TNFAIP8, miR-205-5p could further increase drug sensitivity in the B-RAF^{V600E} mutant melanoma cell lines (Fig. 6B). Moreover, transfection of miR-205-5p in A375 (B-RAF^{V600E} mutant) cells induced the expression of cell apoptotic marker cPARP compared with NC mimic transfected cells (Fig. 6C, lane 1 & 2). Furthermore, transfection of miR-205-5p combined with vemurafenib treatment increased cPARP expression compared with NC mimic transfected and vemurafenib treated cells (Fig. 6C, lane 3 & 4). On the other hand, overexpression of TNFAIP8 decreased paclitaxel and vemurafenib-mediated cPARP expression compared with EV transfected A375 cells (Fig. 6D, compare lanes 1–3 and 4–6). Also, we generated vemurafenib drug-resistant A375R and A2058R melanoma cell lines and utilized in the study. A higher expression of TNFAIP8, autophagy marker LB3 β II, and increased cell proliferation were observed in A375R or A2058R vemurafenib drug-resistant cells compared with parent A375 or A2058 melanoma cells (Fig. 6E,F).

Collectively the data presented in Fig. 6 suggest that (A) expression of miR-205-5p in melanoma cells increases sensitivity towards vemurafenib particularly in B-RAF^{V600E} mutant cells (B) increased expression of TNFAIP8 reduces drug-mediated cell apoptosis, and (C) increased expression of TNFAIP8 due to vemurafenib drug-resistance increases autophagy and cell proliferation. Indeed, our data suggest that TNFAIP8 might be involved in drug resistance in melanoma cell lines by inducing autophagy as reported in prostate and liver cancer cell lines previously^{34,43}, whereas miR-205-5p controls TNFAIP8/autophagy axis and increased sensitivity towards skin cancer drug vemurafenib.

Discussion

In the current study and for the first time, we demonstrate a molecular and mechanistic role of TNFAIP8 in the regulation of skin cancer cell survival/proliferation, colony formation, migration, and drug resistance. Our data was generated by comparison of the normal skin cell-derived cell line (HaCaT) to melanoma cell lines A375, A2058, SK-MEL-2, and the epidermoid carcinoma A431 cell line. TNFAIP8 has been shown to play a role in oncogenesis in several cancers^{32,54} and its expression is induced by inflammatory cytokine TNF α ³⁴. In the current study, we demonstrate that exposure of skin cancer cells with TNF α induced expression of TNFAIP8 that modulates cell proliferation. Similarly, overexpression or knockdown of TNFAIP8 affected cell proliferation in skin cancer cell lines. Mechanistically, TNFAIP8 contains a death effector domain that modulates the caspase-8 activity and negatively regulates apoptosis³². Our preliminary data indicate that TNFAIP8 expression is down-regulated in B-RAF^{V600E} mutant A375, A2058 melanoma cells compared with A431, SK-MEL-2, or normal HaCaT cells which express wild-type B-RAF kinase. However, in skin melanoma patient tissues the expression of TNFAIP8 is higher compared with BCC, SCC, or normal skin tissues indicating that the B-RAF background might play an important role in TNFAIP8 expression in skin cancer and this needs to be further investigated.

This study identified miR-205-5p as a negative regulator of TNFAIP8 gene expression. Other studies have shown that the expression of several miRNAs with established oncogenic roles is upregulated in melanoma cells^{20–24}, whereas particularly miR-205 expression in skin cancer cells is down-regulated also reported in previous studies^{28,55,56}. We found that melanoma cell lines show undetectable levels of miR-205-5p expression as well as higher expression of TNFAIP8 in SK-MEL-2 melanoma cells and melanoma tissue. Further, we demonstrated that miR-205-5p binds with the 3'UTR of TNFAIP8 gene and inhibits TNFAIP8 expression and TNFAIP8-mediated autophagy in skin cancer cells. Previously, we showed that TNFAIP8 mediated induction of autophagy is required for drug resistance and cell survival in prostate cancer cells³⁴ as well as liver cancer cells⁴³, and similarly, in the current study we demonstrated that miR-205-5p controls the expression of TNFAIP8 and TNFAIP8 mediated-autophagy in skin cancer cells. miR-205-5p expression in melanoma cell lines not only controlled the expression of TNFAIP8 but also increased sensitivity towards vemurafenib, a skin cancer drug currently used for the treatment of patients affected by advanced melanoma with B-RAF^{V600E} mutant kinase⁵⁷.

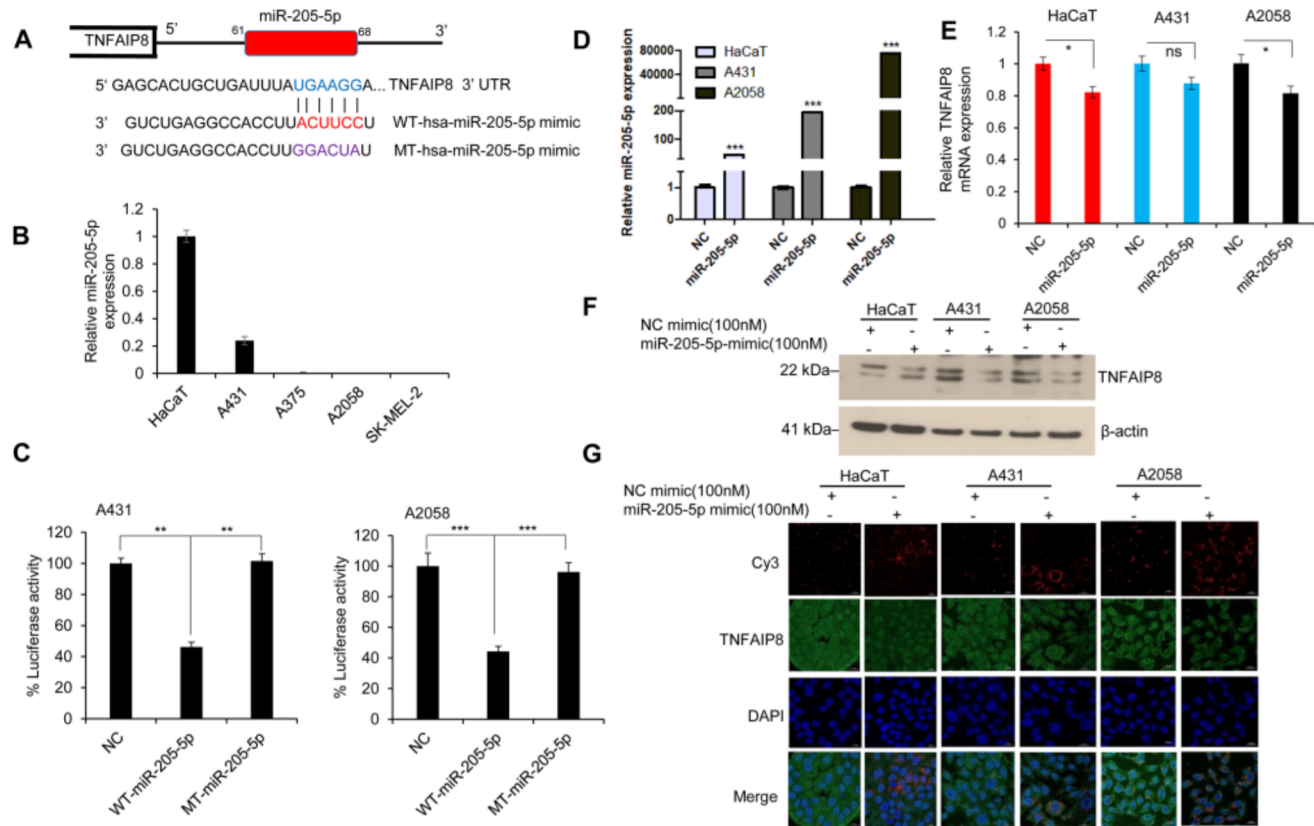


Figure 4. miR-205-5p targets the 3'UTR of TNFAIP8 and inhibits TNFAIP8 expression. (A) The binding site of miR-205-5p in the 3'UTR of TNFAIP8 was analyzed by TargetScan (http://www.targetscan.org/vert_72/) and presented. We also generated a wild type and mutated binding nucleotides of miR-205-5p to the 3'UTR of TNFAIP8. Wild-type miR-205-5p and mutant miR-205-5p mimics are shown. (B) Relative expression of miR-205-5p in HaCaT, A431, A375, A2058, and SK-MEL-2 cell lines was analyzed by RT/qPCR as described in the “Materials and methods” section. (C) Luciferase reporter assay: A431 and A2058 cells were transfected with TNFAIP8-3'UTR-Luciferase reporter construct (0.5 µg) for 18 h and then transfected with NC mimic or wild-type miR-205-5p mimic or mutant miR-205-5p mimic for an additional 24 h. Transfected cells were lysed, and luciferase activity was measured. Results are representative of two independent experiments. **P < 0.01, ***P < 0.001 compared with NC or mutant-type miR-205-5p mimic. (D, E) Normal or skin cancer cells were transfected with NC or miR-205-5p mimic for 48 h and the overexpression of miR-205-5p mimic and TNFAIP8 transcripts were analyzed by RT/qPCR. ***P < 0.001 compared with NC-transfected cells. *P < 0.05 compared with NC-transfected cells. ns-no significance. (F) HaCaT, A431 and A2058 cell lines were transfected with NC mimic or miR-205-5p mimic for 40 h and expression of endogenous TNFAIP8 protein were analyzed by western blotting. Western blots were developed using ECL chemiluminescence detection reagents, the blots were exposed to X-Ray films, scans were converted into grayscale and presented. (G) HaCaT, 431 and A2058 cell lines were grown on a coverslip and transfected with Cy3-labeled NC mimic or Cy3-labeled miR-205-5p mimic and the effect of Cy3-labeled miR-205-5p mimic on endogenous TNFAIP8 expression (green) was visualized by immunofluorescence as described in the “Materials and methods” section.

An earlier study revealed that constitutive activation of B-RAF^{V600E} mutant activates the MEK/ERK pathway and enhances melanoma cell proliferation whereas inhibition of the B-RAF^{V600E} mutant by vemurafenib decreases melanoma cell proliferation⁵⁸. Irrespective of prior treatment with MEK inhibitors or BRAF inhibitor, a recent phase I clinical study demonstrates that vemurafenib, carboplatin, and paclitaxel combination chemotherapy is more effective and tolerable in patients with advanced melanoma with B-RAF^{V600E} mutant protein⁵³. We also showed that inhibition on TNFAIP8 by expression of miR-205-5p drastically decreased vemurafenib-mediated cell proliferation in melanoma cell lines. On the other hand, overexpression of TNFAIP8 reduced vemurafenib or paclitaxel-mediated melanoma cell apoptosis suggests that, TNFAIP8 increased drug resistance in melanoma cell lines by inducing autophagy and by inhibiting cell apoptosis.

Not only the mutation of key oncogenes (*RAS*, *B-RAF*, *MAPK1/2*) involved in skin cancer progression, but reports also suggest that chronic inflammatory pathways regulate the development of melanoma^{59,60}. During chronic inflammation, activation of several transcription factors such as NF- κ B, STAT3, HIF-1-alpha, and up-regulation of their downstream targets including prostaglandins, cyclooxygenase-2 (COX-2), and cytokine TNF- α was reported^{59,60}. TNF- α activates NF- κ B that binds with the TNFAIP8 promoter and induces TNFAIP8 expression^{32,34}. Similarly, our data suggest that the induction of TNFAIP8 by TNF α increases cell proliferation and drug resistance in skin cancer cells.

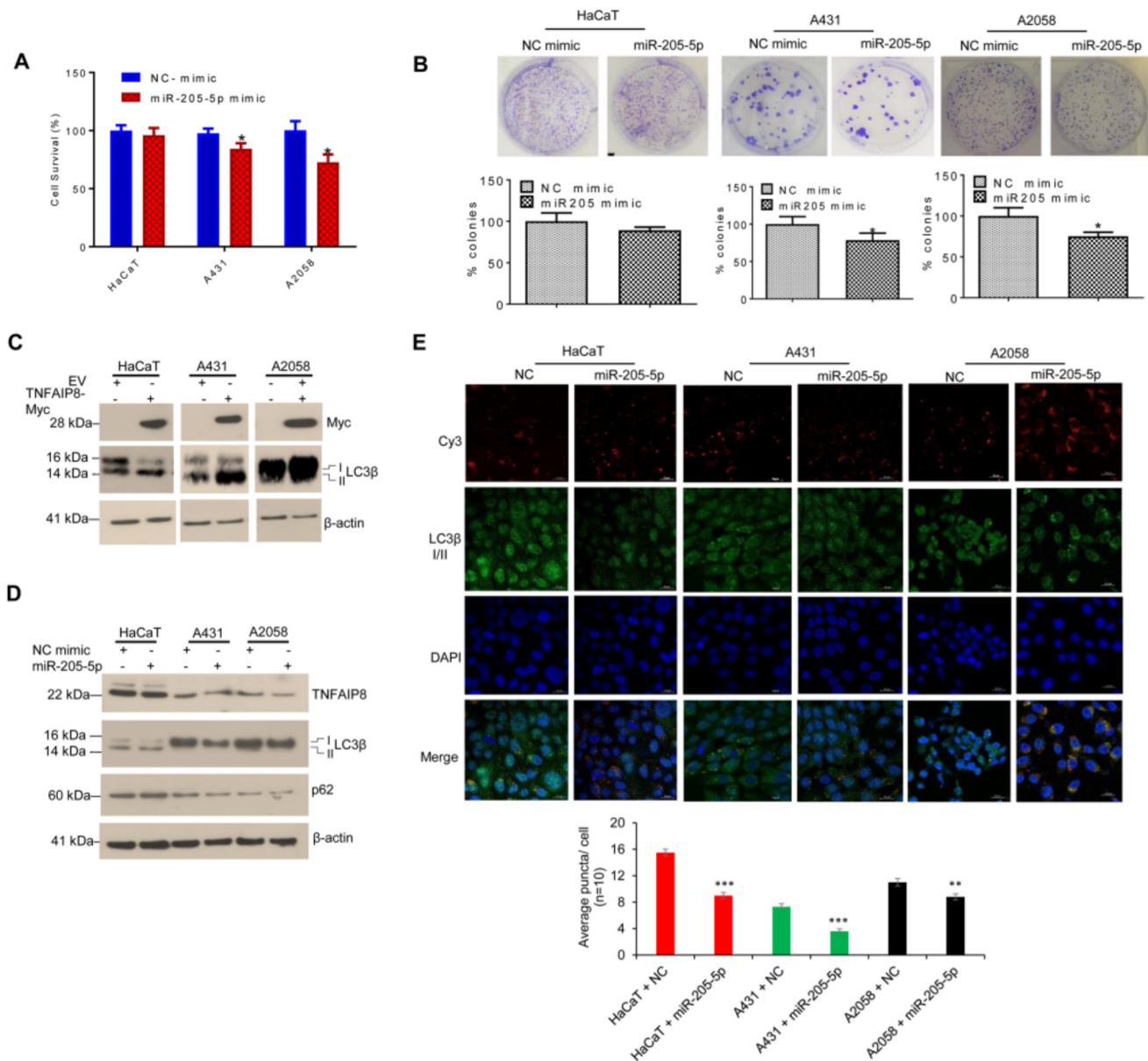


Figure 5. miR-205-5p targets TNFAIP8 and reduces TNFAIP8-mediated cell proliferation and autophagy. (A) HaCaT, A431 and A2058 cells were transfected with NC mimic or miR-205-5p mimic for 48 h and relative cell survival was analyzed by MTT assay. The experiments were independently repeated three times. * $P < 0.05$ compared with NC mimic transfected cells. (B) NC mimic or miR-205-5p mimic transfected cells were re-plated in 6-well plates for 7–10 days and cell colony formation was analyzed and plotted (upper and lower panels) as described in the “Materials and methods” section. The experiment was repeated twice in triplicates. * $P < 0.05$ relative to NC mimic transfected cells. (C) HaCaT, A431 and A2058 cells were transfected EV or TNFAIP8-Myc plasmids for 30 h and lysates were western blotted with anti-Myc, anti-LC3β I/II, and anti-β-actin antibodies. Western blots were developed using ECL chemiluminescence detection reagents, the blots were exposed on X-ray films, converted into grayscale, and presented. (D) HaCaT, lanoma A431 and A2058 cells were transfected NC mimic or miR-205-5p mimic for 30 h and lysates were western blotted with anti-TNFAIP8, anti-LC3β I/II, anti-p62, and anti-β-actin antibodies. Western blots were developed using ECL chemiluminescence detection reagents, exposed on X-Ray films, converted into grayscale, and presented. (E) HaCaT, A431 and A2058 cells were grown on a coverslip transfected with Cy3-labeled NC mimic or Cy3-labeled miR-205-5p mimic and the effect of Cy3-labeled miR-205-5p mimic on endogenous LC3β I/II expression (green) and related puncta formation were visualized by immunofluorescence (upper panel) as described in the “Materials and methods” section (upper panel). LC3β I/II and related puncta were measured from individual cells (n=10) and plotted (lower panels). ** $P < 0.01$, *** $P < 0.001$ relatives to Cy3 labeled-NC mimic transfected cells.

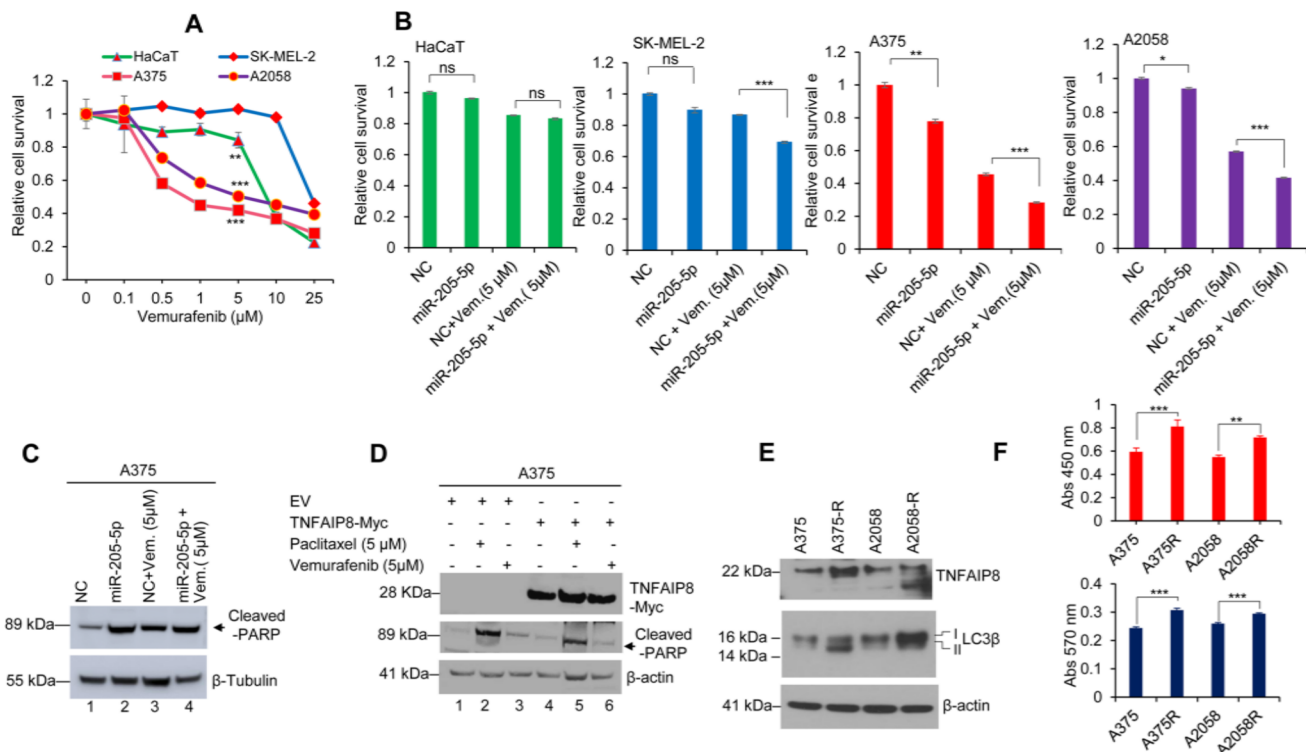


Figure 6. miR-205-5p targets TNFAIP8 in skin cancer cells and increase sensitivity to vemurafenib. **(A)** HaCaT cells, and skin cancer SK-MEL-2, A375 and A2058 cell lines were treated with increasing concentrations of vemurafenib for 48 h and relative cell survival/proliferation was measured by MTT assay. The experiments were independently repeated three times. $^{**}P < 0.01$, $^{***}P < 0.001$ compared to vehicle-treated cells. **(B)** HaCaT cells and skin cancer SK-MEL-2, A375 and A2058 cell lines were transfected with NC mimic or miR-205-5p mimic for 24 h and treated with vemurafenib or vehicle for an additional 48 h and relative cell survival were measured by MTT assay as described in the “Materials and methods” section. $^{*}P < 0.05$, $^{**}P < 0.01$, $^{***}P < 0.001$ compared to NC mimic vehicle-treated cells or NC mimic and vemurafenib-treated cells. ns-no significance. **(C)** Melanoma A375 cells were transfected with NC mimic or miR-205-5p mimic for 18 h and then cells were treated with vemurafenib for an additional 24 h. Fifty micrograms of lysates were immunoblotted with anti-cleaved-PARP and anti-β-tubulin antibodies. Western blots were developed using ECL chemiluminescence detection reagents, the blots were scanned using Azure C-500 Biosystem, scans were converted into grayscale and presented. **(D)** Melanoma A375 cells were transfected with EV of TNFAIP8-Myc plasmid for 18 h first and then cells were treated with vemurafenib or paclitaxel for 24 h as indicated and fifty micrograms lysates were immunoblotted with anti-Myc, anti-cleaved-PARP, and anti-β-actin antibodies. Western blots were developed using ECL chemiluminescence detection reagents and the blots were scanned using an Odyssey CLx imager. The immunoblot scans were converted into grayscale and presented. **(E)** Fifty micrograms of lysates from A375 and A2058 cells or A375R and A2058R (vemurafenib resistant) cells were immunoblotted with anti-TNFAIP8, anti-LC3B I/II, and anti-β-actin antibodies. Western blots were developed using ECL chemiluminescence detection reagents, the blots were exposed on X-Ray films, scans were converted into grayscale and presented. **(F)** Relative cell proliferation/cell survival rate of A375 and A2058 cells, or A375R and A2058R (vemurafenib resistant) cells were measured by using WST-1 reagent (Cayman Chemical) (upper panel) or MTT assay reagent (lower panel) and plotted. $^{**}P < 0.01$, $^{***}P < 0.001$ compared to A375 and A2058 parent cells. Results are representative of three independent experiments. Vem. Vemurafenib.

Since disruption of the p53 pathway was reported in melanoma¹⁴, and recently the role of TNFAIP8 in p53 signaling was analyzed in lung cancer cells and the study revealed that TNFAIP8 variant 2 (v2) represses tumor suppressor wild-type p53 function in lung cancer A549 cells³⁷. Silencing of TNFAIP8 v2 induces p53-independent inhibition of DNA synthesis, widespread p53 binding, the initiation of p53-dependent cell-cycle arrest, and the sensitization of cells to doxorubicin³⁷. Mutant p53 (p53-K120) binds the TNFAIP8 locus at a cryptic p53 response element that is not occupied or bound by wild-type p53 and thus increases TNFAIP8 expression, which promotes lung cancer cell survival/proliferation³⁹. However, the exact role of TNFAIP8 in p53 regulation and signaling in melanoma and other skin cancers remains unknown.

Indeed, for the first time, we report here that TNFAIP8 enhances skin cancer cell proliferation and cell colony formation and migration. By induction of autophagy and by inhibiting cell apoptosis, TNFAIP8 also increased drug resistance in skin cancer cells. Interestingly, we also demonstrated that the expression of miR-205-5p controls the expression of TNFAIP8 and sensitizes melanoma cells to the B-RAF^{V600E} mutant kinase inhibitor vemurafenib.

Materials and methods

Cell culture. Skin cancer A431, A375, A2058, SK-MEL-2 cell lines, and the normal skin HaCaT cell line were obtained from ATCC (Manassas, VA). Cells were grown in DMEM medium (Invitrogen, Carlsbad, CA) containing 5% fetal bovine serum (FBS; Access Biologicals, Vista, CA) and 1% penicillin/streptomycin. Cell lines were maintained at 37 °C in a humidified cell culture incubator containing 5% CO₂. We also generated B-RAF^{V600E} mutant inhibitor vemurafenib resistance A375R and A2058R Cells. A375 and A2058 Cells were treated with 0.5–10 μM of vemurafenib. The cells were passaged twice every week to induce B-RAF^{V600E} mutant inhibitor resistance and drug resistance cells were maintained in 1 μM vemurafenib. All cell lines were grown for at least 24 h and used for experimentation when they reached 70–80% confluence.

Immunohistochemical analysis (IHC) of human skin cancer tissue samples. Skin cancer tissue samples used in the study were gifted from the Department of Pathology, General Hospital of Ningxia Medical University, Yinchuan, Ningxia Hui Autonomous Region, China. The samples included normal skin tissue (n = 6), basal cell carcinoma (BCC) (n = 6), high differentiated squamous cell carcinoma (H-SCC) (n = 4), medium differentiated squamous cell carcinoma (M-SCC) (n = 4), low differentiated squamous cell carcinoma (M-SCC) (n = 4), skin nevus tissues (n = 6), and skin melanoma tissues (n = 6). Paraffin-embedded four-micron tissue sections were prepared and stained with a TNFAIP8 antibody (1:50 dilution) by incubation at 4 °C overnight. TNFAIP8 expression was detected using a Vector Labs Elite ABC Kit with 3,3'-diaminobenzidine as the chromogen and hematoxylin as the counterstain (Innovex Biosciences). Slides were observed under a light microscope and photographed. The relative expression of TNFAIP8 from normal skin tissue and skin cancer tissues was quantified using Image-J software (<https://imagej.nih.gov/ij/>) and an average TNFAIP8 expression density was plotted.

Western blot. Skin cancer A431, A375, A2058, SK-MEL-2 cell lines, and the normal skin HaCaT cell line were grown for 24 h and treated or transfected with indicated plasmids. Transfected or treated cells were lysed in cell lysis buffer (Cell Signaling Technology, Danvers, MA) containing a protease inhibitor cocktail (Roche, Indianapolis, IN) and after centrifugation (10 min at 10,000 rpm) cell supernatant lysates were collected. The protein concentrations were measured from the supernatants using the Bio-Rad protein assay reagent (Bio-Rad, Hercules, CA). Western blotting was performed as described previously³⁴. In short, cell lysates (50 μg) were separated on NuPAGE 4–12% Bis–Tris-SDS gels (Invitrogen) and then transferred to a polyvinylidene difluoride (PVDF) membrane (Millipore, Billerica, MA). The membranes were blocked in 1X blocking buffer (Sigma-Aldrich, St. Louis, MO) and incubated with primary antibodies overnight at 4 °C. The following antibodies were obtained from Cell Signaling Technology (Danvers, MA): anti-B-RAF, anti-LC3β I/II, anti-p62, anti-Myc tag, anti-Cleaved-PARP, anti-β-tubulin, and anti-GAPDH. Anti-β-actin antibody from Sigma (St. Louis, MO) and anti-TNFAIP8 antibody from Proteintech Group (Rosemont, IL) was also purchased. All primary antibodies were used as per the manufacturer's suggestions, typically at a 1:1000 dilution. After washing the membranes three times, the membranes were incubated in the appropriate secondary antibody conjugated with HRP (1:10,000 dilution) (Jackson ImmunoResearch, PA) or anti-rabbit secondary antibody conjugated with IRDye-680RD (LI-COR) for 1 h at room temperature, and immunoreactive bands were visualized using ECL chemiluminescence detection reagents (Signagen Laboratories, Rockville, MD) or by scanning the blots with an Odyssey CLx imager. The immunoblot scans were converted into grayscale and presented. The original immunoblot scans were presented as Supplementary Figs. S2–S7 with the manuscript.

Cell transfection. Empty vector (EV) pcDNA3.1 or TNFAIP8 (human tumor necrosis factor-alpha-induced protein eight transcript variant 1)-Myc-DDK-tagged ORF cDNA plasmid was obtained from Origene (Rockville-MD, Cat # RC202729). Skin cancer A431, A375, and A2058 or HaCaT cell lines were grown in 6-well plates (1 × 10⁵ cells/wells) for 24 h before transfection and 2 μg of EV or TNFAIP8-Myc tagged plasmid DNA was transfected using Lipofectamine LTX Plus transfection reagent (Invitrogen). After 30–40 h of transfection, cells were harvested, and the expression of the TNFAIP8-Myc tagged protein was examined by immunoblotting. For siRNA transfection, control siRNA and human TNFAIP8 siRNA were obtained from Dharmacon (Lafayette, CO). Skin cancer A431, A375, and A2058 or normal skin cells were grown in antibiotic-free medium overnight and transfected with 100 nM control or TNFAIP8 siRNA using Lipofectamine RNAiMAX reagent (Invitrogen). For miRNA transfection, negative control (NC) and miR-205-5p mimic miRNAs were obtained from Origene (Rockville-MD) and skin cancer cells or normal skin cells were transfected with NC or miR-205-5p mimic microRNAs (100 nM) using Lipofectamine-2000 reagent (Invitrogen). After transfection of 30 h, cells were harvested and expression of miR-205-5p or TNFAIP8 was analyzed.

RT/PCR and RT/qPCR. Total RNA from skin cancer SK-MEL-2, A431, A375, A2058, and HaCaT cell lines was isolated using TRIZOL reagent (Life Technologies), and after cDNA synthesis, the expression of TNFAIP8 isoforms was amplified by PCR by using isoform-specific primers (Supplementary Table S1) followed by RT/PCR as described previously³⁴. The PCR products were electrophoresed on a 1.5% agarose gel stained with ethidium bromide. The PCR-amplified bands were extracted from the agarose gel and sequenced to confirm the identity of the isoforms. In other experiments, skin cancer A431, A375, A2058, and normal skin HaCaT cells were treated with TNFα (20 ng/ml) for 30 h and total RNA from cells was isolated using TRIZOL reagent. Equal amounts of RNA (1 μg) was reverse transcribed using a High Capacity cDNA Reverse Transcription kit (Applied Biosystems), and cDNA was incubated with Power SYBR Green PCR master mix (Applied Biosystems) and mixed with forward and reverse primers of TNFAIP8 (Supplementary Table S1). GAPDH primers were used as an internal control. For miR-205-5p expression analysis, total microRNAs from normal or skin cancer cells

were isolated using the mirVana microRNA Isolation Kit (Thermo Fisher Scientific). Total miRNAs (10 ng) were reverse transcribed using primers specific for miR-205-5p and U44 (Assay IDs 000509 and 001094, Applied Biosystems, Carlsbad, CA) and TaqMan Reverse Transcription reagents (Applied Biosystems). Expression of miR-205-5p and U44 was quantified by RT/qPCR using TaqMan PCR master mixture and Taqman expression assay primers. U44 expression was used as an internal control. The PCR reactions were run on a QuantStudio-3 PCR system (Applied Biosystems) and relative quantitation was analyzed according to the manufacturer's protocols.

Cell survival MTT assay. Skin cancer A431, A375, A2058 and, normal skin HaCaT cells (1×10^4 cells/well) were grown in 96 plates for 18 h. Cells were treated with different concentrations of TNF α for 48 h and relative cell survival was analyzed by MTT 3-(4,5-dimethylthiazol-2-yl)-2,5-diphenyltetrazolium bromide (MTT) reagent (MP Biochemicals, Santa Ana, CA). Similarly, in other experiments, skin cancer cells or normal skin cells (1×10^5) were seeded onto 6-well plates for 24 h and transfected with EV of TNFAIP8-Myc plasmids or control siRNA and TNFAIP8 siRNA separately for 24 h. The transfected cells were harvested, and ten thousand cells seeded onto 96-well plates 48 h. Cells were incubated with 5 μ l/well of MTT reagent (5 mg/ml) for 1 h at 37 °C in a cell culture incubator. Cells were washed with PBS, formazan crystals were dissolved in DMSO, and cell survival was quantified by reading the plates at 570 nm using a Fluostar Omega plate reader (BMG Lab Tech, Cary, NC).

Colony formation assay. Skin cancer A431, A375, A2058, and normal skin HaCaT cells (1×10^5 cells/well) were grown in six plates for 18 h and cells were transiently transfected with TNFAIP8-Myc plasmid or empty-vector (EV) (2 μ g/well in 6-well plates), or TNFAIP8 siRNA or control siRNA as indicated in different figures. In other experiments, cells were transfected with NC mimic or miR-205-5p mimic miRNAs for 24 h. Transfected cells were trypsinized and counted and live cells (3000 cells/well) were re-plated in 6-well plates in triplicate and allowed to grow for 7–10 days. Cells were washed with PBS, fixed with cold methanol, and stained with 0.1% crystal violet for 1 h. Cells were washed with distilled water and allowed to dry. Blue colonies were counted and plotted.

Migration assay. The effect of miR-205-5p overexpression on the migratory ability of skin cancer cells was analyzed by a wound healing migration assay as described previously¹⁷. Cells were transfected with miR-205-5p or NC mimic and transfected cells were plated, and the cell monolayer was scraped using a micropipette tip (A_0). At 24 h post-wounding (A_{24}), cells were photographed, and the migration gap length was calculated using ImageJ software (<https://imagej.nih.gov/ij/>). The percent wound closure was calculated using the formula $[(A_0 - A_{24})/A_0] \times 100$.

Immunofluorescence. HaCaT cells and skin cancer cell lines A431 and A2058 (1.5×10^5) were grown on coverslips in 6-well plates and transfected with custom made Cy3-labeled NC or miR-205-5p mimic (Bioneer, Oakland, CA) for 48 h. After washing with PBS, cells were fixed with paraformaldehyde (4%) for 15 min, permeabilized with 0.25% Triton X-100 in PBS, and blocked with 2% bovine serum albumin in PBS for 1 h at room temperature. Cells were washed with PBS two times (15 min each) and incubated with anti-TNFAIP8 or anti-LB3 β I/II rabbit primary antibodies (diluted 1:500) at 4 °C for 18 h. Cells were washed again twice with PBS and incubated with Alexa-Fluor 488-conjugated fluorescein-labeled anti-rabbit secondary antibody (Invitrogen). After the immunostaining, cells were washed three times with PBS mounted with Vectashield-DAPI mounting medium (Vector Laboratories, Burlingame, CA, Cat # H-1500-10). Slides were observed under a confocal microscope ZEISS LS 800 and images were captured.

Luciferase assay. For luciferase assay, first A431 and A2058 melanoma cells were transfected with 1 μ g of TNFAIP8-3'UTR-Luciferase reporter construct (OriGene) in 96 well plates. After 18 h of transfection, cells were further transfected with 100 nM of miR-205-5p (wild-type), or miR-205-5p (mutant) mimic or NC mimic miRNAs for an additional 24 h. Transfected cells were washed with PBS and mixed with luciferase substrate (Switchgear Genomics, Carlsbad, CA, Cat # LS010). Plates were covered with aluminum foil to protect from light and incubated at room temperature for 30 min. The plates were read by using Fluostar Omega plate reader (BMG Lab Tech, Cary, NC) and relative luciferase activity was measured and plotted.

Statistical analysis. Results are from independent duplicate or triplicate experiments and presented as means \pm SEM. Differences between groups were analyzed using either two-tailed Student's *t* test or one-way ANOVA followed by Tukey HSD post-hoc test. A *P* value of < 0.05 was considered statistically significant. Statistical analyses were performed using the IBM SPSS Statistics 25 software (NY, USA) or Graph Pad Prism (Version: 8 GraphPad Software Inc., CA, USA).

Data availability

All data produced during the current study are included in this article and its “Supplementary files”.

Received: 18 July 2020; Accepted: 14 January 2021

Published online: 11 March 2021

References

- Whiteman, D. C., Green, A. C. & Olsen, C. M. The growing burden of invasive melanoma: Projections of incidence rates and numbers of new cases in six susceptible populations through 2031. *J Invest. Dermatol.* **136**, 1161–1171. <https://doi.org/10.1016/j.jid.2016.01.035> (2016).
- de Vries, E. & Coebergh, J. W. Cutaneous malignant melanoma in Europe. *Eur. J. Cancer* **40**, 2355–2366. <https://doi.org/10.1016/j.ejca.2004.06.003> (2004).
- Rogers, H. W., Weinstock, M. A., Feldman, S. R. & Coldiron, B. M. Incidence estimate of nonmelanoma skin cancer (Keratinocyte Carcinomas) in the US Population, 2012. *JAMA Dermatol.* **151**, 1081–1086. <https://doi.org/10.1001/jamadermatol.2015.1187> (2015).
- Mansouri, B. & Housewright, C. D. The treatment of actinic keratoses—the rule rather than the exception. *JAMA Dermatol.* **153**, 1200. <https://doi.org/10.1001/jamadermatol.2017.3395> (2017).
- Merlino, G. *et al.* The state of melanoma: Challenges and opportunities. *Pigment Cell Melanoma Res.* **29**, 404–416. <https://doi.org/10.1111/pcmr.12475> (2016).
- Apalla, Z., Nashan, D., Weller, R. B. & Castellsague, X. Skin cancer: Epidemiology, disease burden, pathophysiology, diagnosis, and therapeutic approaches. *Dermatol. Ther. (Heidelb.)* **7**, 5–19. <https://doi.org/10.1007/s13555-016-0165-y> (2017).
- Saladi, R. N. & Persaud, A. N. The causes of skin cancer: A comprehensive review. *Drugs Today (Barc.)* **41**, 37–53. <https://doi.org/10.1358/dot.2005.41.1.875777> (2005).
- Bradford, P. T. Skin cancer in skin of color. *Dermatol. Nurs.* **21**, 170–177 (2009) (206; quiz 178).
- Montagna, W. & Carlisle, K. The architecture of black and white facial skin. *J. Am. Acad. Dermatol.* **24**, 929–937. [https://doi.org/10.1016/0190-9622\(91\)70148-u](https://doi.org/10.1016/0190-9622(91)70148-u) (1991).
- Hussein, M. R. Ultraviolet radiation and skin cancer: Molecular mechanisms. *J. Cutan. Pathol.* **32**, 191–205. <https://doi.org/10.111/j.0303-6987.2005.00281.x> (2005).
- Trucco, L. D. *et al.* Ultraviolet radiation-induced DNA damage is prognostic for outcome in melanoma (vol 25, pg 221, 2018). *Nat. Med.* **25**, 350–350. <https://doi.org/10.1038/s41591-018-0325-y> (2019).
- Sample, A. *et al.* The autophasy receptor adaptor p62 is Up-regulated by UVA radiation in melanocytes and in melanoma cells. *Photochem. Photobiol.* **94**, 432–437. <https://doi.org/10.1111/php.12809> (2018).
- Hayward, N. K. *et al.* Whole-genome landscapes of major melanoma subtypes. *Nature* **545**, 175–180. <https://doi.org/10.1038/nature22071> (2017).
- Shain, A. H. *et al.* Genomic and transcriptomic analysis reveals incremental disruption of key signaling pathways during melanoma evolution. *Cancer Cell* **34**, 45–55.e44. <https://doi.org/10.1016/j.ccr.2018.06.005> (2018).
- Polksy, D. & Cordon-Cardo, C. Oncogenes in melanoma. *Oncogene* **22**, 3087–3091. <https://doi.org/10.1038/sj.onc.1206449> (2003).
- Kunz, M. Oncogenes in melanoma: An update. *Eur. J. Cell Biol.* **93**, 1–10. <https://doi.org/10.1016/j.ejcb.2013.12.002> (2014).
- Cagle, P. *et al.* MicroRNA-214 targets PTK6 to inhibit tumorigenic potential and increase drug sensitivity of prostate cancer cells. *Sci. Rep.* **9**, 9776. <https://doi.org/10.1038/s41598-019-46170-3> (2019).
- Bartel, D. P. MicroRNAs: Genomics, biogenesis, mechanism, and function. *Cell* **116**, 281–297 (2004).
- Greenberg, E. S., Chong, K. K., Huynh, K. T., Tanaka, R. & Hoon, D. S. Epigenetic biomarkers in skin cancer. *Cancer Lett.* **342**, 170–177. <https://doi.org/10.1016/j.canlet.2012.01.020> (2014).
- Penna, E. *et al.* microRNA-214 contributes to melanoma tumour progression through suppression of TFAP2C. *EMBO J.* **30**, 1990–2007. <https://doi.org/10.1038/embj.2011.102> (2011).
- Gaziel-Sovran, A. *et al.* miR-30b/30d regulation of GalNAc transferases enhances invasion and immunosuppression during metastasis. *Cancer Cell* **20**, 104–118. <https://doi.org/10.1016/j.ccr.2011.05.027> (2011).
- Streicher, K. L. *et al.* A novel oncogenic role for the miRNA-506-514 cluster in initiating melanocyte transformation and promoting melanoma growth. *Oncogene* **31**, 1558–1570. <https://doi.org/10.1038/onc.2011.345> (2012).
- Grignol, V. *et al.* miR-21 and miR-155 are associated with mitotic activity and lesion depth of borderline melanocytic lesions. *Br. J. Cancer* **105**, 1023–1029. <https://doi.org/10.1038/bjc.2011.288> (2011).
- Kanemaru, H. *et al.* The circulating microRNA-221 level in patients with malignant melanoma as a new tumor marker. *J. Dermatol. Sci.* **61**, 187–193. <https://doi.org/10.1016/j.jdermsci.2010.12.010> (2011).
- Nguyen, T. *et al.* Downregulation of microRNA-29c is associated with hypermethylation of tumor-related genes and disease outcome in cutaneous melanoma. *Epigenetics* **6**, 388–394. <https://doi.org/10.4161/epi.6.3.14056> (2011).
- Mazar, J. *et al.* Epigenetic regulation of microRNA genes and the role of miR-34b in cell invasion and motility in human melanoma. *PLoS ONE* **6**, e24922. <https://doi.org/10.1371/journal.pone.0024922> (2011).
- Mazar, J., DeBlasio, D., Govindarajan, S. S., Zhang, S. & Perera, R. J. Epigenetic regulation of microRNA-375 and its role in melanoma development in humans. *FEBS Lett.* **585**, 2467–2476. <https://doi.org/10.1016/j.febslet.2011.06.025> (2011).
- Dar, A. A. *et al.* miRNA-205 suppresses melanoma cell proliferation and induces senescence via regulation of E2F1 protein. *J. Biol. Chem.* **286**, 16606–16614. <https://doi.org/10.1074/jbc.M111.227611> (2011).
- Freundt, E. C., Bidere, N. & Lenardo, M. J. A different TIPE of immune homeostasis. *Cell* **133**, 401–402. <https://doi.org/10.1016/j.cell.2008.04.017> (2008).
- Kumar, D., Whiteside, T. L. & Kasid, U. Identification of a novel tumor necrosis factor-alpha-inducible gene, SCC-S2, containing the consensus sequence of a death effector domain of fas-associated death domain-like interleukin-1beta-converting enzyme-inhibitory protein. *J. Biol. Chem.* **275**, 2973–2978. <https://doi.org/10.1074/jbc.275.4.2973> (2000).
- Sun, H. *et al.* TIPE2, a negative regulator of innate and adaptive immunity that maintains immune homeostasis. *Cell* **133**, 415–426. <https://doi.org/10.1016/j.cell.2008.03.026> (2008).
- Niture, S. *et al.* Oncogenic role of tumor necrosis factor alpha-induced protein 8 (TNFAIP8). *Cells* <https://doi.org/10.3390/cells8010009> (2018).
- Horrevoets, A. J. *et al.* Vascular endothelial genes that are responsive to tumor necrosis factor-alpha in vitro are expressed in atherosclerotic lesions, including inhibitor of apoptosis protein-1, stannin, and two novel genes. *Blood* **93**, 3418–3431 (1999).
- Niture, S. *et al.* TNFAIP8 promotes prostate cancer cell survival by inducing autophagy. *Oncotarget* **9**, 26884–26899. <https://doi.org/10.18633/oncotarget.25529> (2018).
- Day, T. F. *et al.* Transcriptome and proteome analyses of TNFAIP8 knockdown cancer cells reveal new insights into molecular determinants of cell survival and tumor progression. *Methods Mol. Biol.* **1513**, 83–100. https://doi.org/10.1007/978-1-4939-6539-7_7 (2017).
- Niture, S., Moore, J. & Kumar, D. TNFAIP8: Inflammation, immunity and human diseases. *J. Cell Immunol.* **1**, 29–34 (2019).
- Lowe, J. M. *et al.* The novel p53 target TNFAIP8 variant 2 is increased in cancer and offsets p53-dependent tumor suppression. *Cell Death Differ.* **24**, 181–191. <https://doi.org/10.1038/cdd.2016.130> (2017).
- Wang, L., Song, Y. & Men, X. Variance of TNFAIP8 expression between tumor tissues and tumor-infiltrating CD4+ and CD8+ T cells in non-small cell lung cancer. *Tumour Biol.* **35**, 2319–2325. <https://doi.org/10.1007/s13277-013-1307-9> (2014).
- Monteith, J. A. *et al.* A rare DNA contact mutation in cancer confers p53 gain-of-function and tumor cell survival via TNFAIP8 induction. *Mol. Oncol.* **10**, 1207–1220. <https://doi.org/10.1016/j.molonc.2016.05.007> (2016).
- Han, Y., Tang, Z., Zhao, Y., Li, Q. & Wang, E. TNFAIP8 regulates Hippo pathway through interacting with LATS1 to promote cell proliferation and invasion in lung cancer. *Mol. Carcinog.* **57**, 159–166. <https://doi.org/10.1002/mc.22740> (2018).

41. Zhang, C. *et al.* Role of SCC-S2 in experimental metastasis and modulation of VEGFR-2, MMP-1, and MMP-9 expression. *Mol. Ther.* **13**, 947–955. <https://doi.org/10.1016/j.ymthe.2005.11.020> (2006).
42. Dong, Q. *et al.* TNFAIP8 interacts with LATS1 and promotes aggressiveness through regulation of Hippo pathway in hepatocellular carcinoma. *Oncotarget* **8**, 15689–15703. <https://doi.org/10.18632/oncotarget.14938> (2017).
43. Niture, S. *et al.* TNFAIP8 regulates autophagy, cell steatosis, and promotes hepatocellular carcinoma cell proliferation. *Cell Death Dis.* **11**, 178. <https://doi.org/10.1038/s41419-020-2369-4> (2020).
44. Gao, H. Y., Huo, F. C., Wang, H. Y. & Pei, D. S. MicroRNA-9 inhibits the gastric cancer cell proliferation by targeting TNFAIP8. *Cell Prolif.* <https://doi.org/10.1111/cpr.12331> (2017).
45. Sun, Z. *et al.* TNFAIP8 overexpression: A potential predictor of lymphatic metastatic recurrence in pN0 esophageal squamous cell carcinoma after Ivor Lewis esophagectomy. *Tumour Biol.* **37**, 10923–10934. <https://doi.org/10.1007/s13277-016-4978-1> (2016).
46. Hadisaputri, Y. E. *et al.* TNFAIP8 overexpression: Clinical relevance to esophageal squamous cell carcinoma. *Ann. Surg. Oncol.* **19**(Suppl 3), S589–596. <https://doi.org/10.1245/s10434-011-2097-1> (2012).
47. Liu, K. *et al.* Expression of tumor necrosis factor-alpha-induced protein 8 in pancreas tissues and its correlation with epithelial growth factor receptor levels. *Asian Pac. J. Cancer Prev.* **13**, 847–850 (2012).
48. Talantov, D. *et al.* Novel genes associated with malignant melanoma but not benign melanocytic lesions. *Clin. Cancer Res.* **11**, 7234–7242. <https://doi.org/10.1158/1078-0432.CCR-05-0683> (2005).
49. Ahn, J. H., Han, B. I. & Lee, M. Induction of resistance to BRAF inhibitor is associated with the inability of Spry2 to inhibit BRAF-V600E activity in BRAF mutant cells. *Biomol. Ther. (Seoul)* **23**, 320–326. <https://doi.org/10.4062/biomolther.2015.007> (2015).
50. Yu, H. *et al.* Identification of coexistence of BRAF V600E mutation and EZH2 gain specifically in melanoma as a promising target for combination therapy. *J. Transl. Med.* **15**, 243. <https://doi.org/10.1186/s12967-017-1344-z> (2017).
51. Lin, K. *et al.* The role of B-RAF mutations in melanoma and the induction of EMT via dysregulation of the NF-kappaB/Snail/RKIP/PTEN circuit. *Genes Cancer* **1**, 409–420. <https://doi.org/10.1177/1947601910373795> (2010).
52. Bhatia, P., Friedlander, P., Zakaria, E. A. & Kandil, E. Impact of BRAF mutation status in the prognosis of cutaneous melanoma: An area of ongoing research. *Ann. Transl. Med.* **3**, 24. <https://doi.org/10.3978/j.issn.2305-5839.2014.12.05> (2015).
53. Bhatty, M. *et al.* Phase 1 study of the combination of vemurafenib, carboplatin, and paclitaxel in patients with BRAF-mutated melanoma and other advanced malignancies. *Cancer* **125**, 463–472. <https://doi.org/10.1002/cncr.31812> (2019).
54. Padmavathi, G. *et al.* Novel tumor necrosis factor-alpha induced protein eight (TNFAIP8/TIPE) family: Functions and downstream targets involved in cancer progression. *Cancer Lett.* **432**, 260–271. <https://doi.org/10.1016/j.canlet.2018.06.017> (2018).
55. Sanchez-Sendra, B. *et al.* Downregulation of intratumoral expression of miR-205, miR-200c and miR-125b in primary human cutaneous melanomas predicts shorter survival. *Sci. Rep.* **8**, 17076. <https://doi.org/10.1038/s41598-018-35317-3> (2018).
56. Babapoor, S. *et al.* Identification of microRNAs associated with invasive and aggressive phenotype in cutaneous melanoma by next-generation sequencing. *Lab. Invest.* **97**, 636–648. <https://doi.org/10.1038/labinvest.2017.5> (2017).
57. Chapman, P. B. *et al.* Improved survival with vemurafenib in melanoma with BRAF V600E mutation. *N. Engl. J. Med.* **364**, 2507–2516. <https://doi.org/10.1056/NEJMoa1103782> (2011).
58. Swaika, A., Crozier, J. A. & Joseph, R. W. Vemurafenib: An evidence-based review of its clinical utility in the treatment of metastatic melanoma. *Drug Des. Devel. Ther.* **8**, 775–787. <https://doi.org/10.2147/DDDT.S31143> (2014).
59. Maru, G. B., Gandhi, K., Ramchandani, A. & Kumar, G. The role of inflammation in skin cancer. *Adv. Exp. Med. Biol.* **816**, 437–469. https://doi.org/10.1007/978-3-0348-0837-8_17 (2014).
60. Tang, L. & Wang, K. Chronic inflammation in skin malignancies. *J. Mol. Signal.* **11**, 2. <https://doi.org/10.5334/jmolsig.2017-2187-11-2> (2016).

Acknowledgements

We gratefully acknowledge the Grants U01CA194730, U54MD012392, and R01MD012767 from the National Institutes of Health awarded to D.K and National Natural Science Foundation of China Grant 81641106 to XG.

Author contributions

X.G. and S.N. planned, designed, and performed the experiments and wrote the manuscript. M.L. and P.C. performed the experiments and P.A.L. edited the manuscript and involved in the discussion. D.K. supervised, planned, and designed the research and wrote the manuscript. All authors read and approved the final manuscript.

Competing interests

The authors declare no competing interests.

Additional information

Supplementary Information The online version contains supplementary material available at <https://doi.org/10.1038/s41598-021-85097-6>.

Correspondence and requests for materials should be addressed to S.N. or D.K.

Reprints and permissions information is available at www.nature.com/reprints.

Publisher's note Springer Nature remains neutral with regard to jurisdictional claims in published maps and institutional affiliations.



Open Access This article is licensed under a Creative Commons Attribution 4.0 International License, which permits use, sharing, adaptation, distribution and reproduction in any medium or format, as long as you give appropriate credit to the original author(s) and the source, provide a link to the Creative Commons licence, and indicate if changes were made. The images or other third party material in this article are included in the article's Creative Commons licence, unless indicated otherwise in a credit line to the material. If material is not included in the article's Creative Commons licence and your intended use is not permitted by statutory regulation or exceeds the permitted use, you will need to obtain permission directly from the copyright holder. To view a copy of this licence, visit <http://creativecommons.org/licenses/by/4.0/>.

© The Author(s) 2021